Experimental demonstration of a novel Gas Switching Combustion reactor for power production with integrated CO_2 capture

Abdelghafour Zaabout[1,3], Schalk Cloete[2], Stein Tore Johansen[1], Martin van Sint Annaland[3], Fausto Gallucci[3] & Shahriar Amini[1]

1) Flow Technology Department, SINTEF Materials and Chemistry, Norway

2) Norwegian University of Science and Technology (NTNU), Norway

3) Chemical Process Intensification, Department of Chemical Engineering and Chemistry, Eindhoven University of Technology (TU/e), the Netherlands

1 Abstract

This paper experimentally demonstrates the feasibility of a novel Gas Switching Combustion (GSC) reactor as an alternative to the traditional Chemical Looping Combustion (CLC) process for power production with integrated CO_2 capture. Whereas the CLC process circulates an oxygen carrier material between two fluidized bed reactors where it is exposed to separate fuel and air streams, the GSC concept employs a single dense fluidized bed reactor where the oxygen carrier is periodically exposed to fuel and air streams. A lab-scale GSC reactor was operated autothermally (without any external temperature supply) to continuously convert cold feed gasses into hot product gasses which would be suitable for driving a downstream power cycle. A parametric study was carried out to further investigate the behaviour of the GSC concept. The reactor achieved a high CO_2 capture efficiency (97.2%) and purity (98.2%) even without the use of a purging stage between the oxidation and reduction stages. A small amount of carbon deposition (around 1%) had a slight negative effect on the CO_2 capture efficiency. Finally, the operation of a cluster of GSC reactors capable of delivering two steady process streams to downstream process equipment was discussed.

2 Introduction

Since the start of the second industrial revolution, fossil fuels have driven the global economy to expand by a factor of 50 (1), leading to a 500% increase in population and an 800% increase in per-capita consumption. Today, 150 years later, the global economy remains totally dependent on fossil fuels, deriving fully 87% (2) of its primary energy consumption from oil, coal and natural gas. Fossil fuel consumption is still rapidly increasing while the use of renewable energy sources (primarily hydroelectricity) still contributes only 8% to the global energy production. All major energy roadmaps (3-6) project this trend to continue up to 2030 and beyond.

As a result of the continued increase in fossil fuel combustion (especially the 56% global increase in coal consumption over the decade following China's inclusion in the world trade organization (2)) greenhouse gas emissions are currently following the most pessimistic scenarios outlined by the IPCC in the year 2000. The most recent energy outlook from the International Energy Agency states that long-term atmospheric CO_2 concentrations will reach 660 ppm even under the New Policies Scenario which assumes strong policy action to combat climate change (4). This scenario grants only a 6% chance of staying below 2°C of long-term warming (4) – a threshold generally considered to afford a reasonable chance of not activating catastrophic self-reinforcing global warming (although arguably the world's most renowned climate scientist, James Hansen, calls this threshold "a recipe for long-term disaster"). It is therefore vital that greenhouse gas emissions are curbed through conservation, efficiency and low-carbon energy systems.

Carbon (dioxide) Capture and Storage (CCS) is increasingly seen as an essential technology for accommodating the world's total reliance on fossil fuels while minimizing the potentially catastrophic long-term impacts of climate change (7, 8). However, first generation CCS technologies (mainly based on amine scrubbing) impose a high energy penalty on the system, thereby reducing the efficiency of a fossil fuel power plant by 14-40% (9). This inefficiency significantly increases the price of electricity and also results in wasteful utilization of dwindling stores of easily accessible conventional fossil fuels. A second generation of CO_2 capture technologies is therefore currently being developed with the primary purpose of greatly reducing this energy penalty.

Chemical Looping Combustion (CLC) has recently emerged as one of the most promising of these second generation technologies (10-12). The standard CLC configuration consists of two interconnected reactors: an air and a fuel reactor. A particulate oxygen carrier circulates between these reactors, fulfilling the role of the air separation unit in a standard oxy-fuel CO_2 capture process. As in any oxy-fuel process, contact between the fuel and nitrogen in air is inherently avoided, thereby producing a pure CO_2 stream (after water separation) from the fuel reactor, ready for compression and storage. The CLC process is also capable of achieving virtually 100% CO_2 capture efficiency (as opposed to around 90% from pre- and post-combustion technologies).

Through the use of the solid oxygen carrier material, the CLC process can dramatically reduce the energy penalty associated with air separation in a standard oxy-fuel process. It even displays a thermodynamic advantage over standard one-step combustion processes, thereby allowing for improved plant efficiency (13). As a result, a coal-fired CLC process can theoretically result in close to 100% CO_2 capture while generating electricity at a higher efficiency than an ultra-supercritical coal plant (14) – a very promising prospect indeed. It has been estimated that such a CLC plant would impose a CO_2 avoidance cost as low as €10/ton (15).

The development and selection of suitable oxygen carrier materials has thus far been the top CLC research priority (16, 17), but research attention is increasingly being paid to actually employing these materials in Circulating Fluidised Beds (CFBs) under the standard CLC configuration (18, 19). This configuration has been demonstrated experimentally at lab and small pilot scales in several studies (20-22), but is facing many technical and operational difficulties which arise mainly from the interconnected reactor configuration. Solids circulation between the two reactors requires costly particle separation systems together with loop seals to prevent gas leakage. Particle separation can be particularly expensive due to the capital costs and pressure losses associated with high-volume high-temperature

cyclones and the degradation of the oxygen carrier material under separation. The interconnected nature of the standard CLC setup also introduces significant uncertainties regarding process scale-up, thereby requiring many years of incremental scale-up, testing and demonstration. Pressurized operation of the standard CLC system is also practically very challenging.

As an alternative, Noorman et al. (23, 24) proposed a CLC system working in switching mode under packed bed conditions. In this new concept, inlet gasses (air and fuel) are fed periodically to a packed bed of oxygen carrier material, thereby avoiding any solids circulation since the two stages, oxidation and reduction, occur in a single reactor. The lab-scale reactor has shown promising results even while greatly reducing process complexity. In addition, it also allows for high pressure operation and facilitates direct heat integration between the two process stages.

Despite these large benefits, however, a number of drawbacks related to the packed bed can also be identified. Problems can arise with the stability and reactive performance of manufactured packed bed pellets, and, most importantly, the large axial temperature gradients developing within the packed bed as the reaction front moves through the reactor can cause stability problems to the oxygen carrier. If cold gas is fed to the reactor, the solids material closest to the inlet will be continuously cooled down once the reaction front has moved past that position. As a result, these solids could be too cold to react in the next process stage. Some solutions are believed to overcome this issue, which are i) the use of an oxygen carrier that is highly reactive at lower temperatures as first part of the reactor (25), ii) design an appropriate strategy of heat management of the reactor (26). However this latter could lead to a slight decrease of the overall efficiency of the plant in some cases.

Despite these drawbacks, however, this switching mechanism has great potential to reduce the capital costs, increase process efficiency and accelerate the scale-up of the CLC concept. For this reason, this study will experimentally evaluate the switching concept in a bubbling fluidized bed reactor – a concept henceforth referred to as Gas Switching Combustion (GSC). The excellent mixing occurring in bubbling fluidized beds automatically eliminates the problem with large axial temperature gradients described above. It also eliminates the possibility of hot-spot formation in the highly exothermic oxidation stage. In addition, cheap natural mineral ore can be used directly in the bubbling fluidized bed and continuous replenishment of this cheap oxygen carrier material would be possible. The bubbling fluidized bed will also allow for lower pressure drops and higher gas feed rates while maintaining the easy scalability, good heat integration and possibility for high pressure operation allowed by the packed bed concept.

Motivated by these advantages, the feasibility of the GSC concept is experimentally demonstrated in this paper by achieving autothermal operation in a lab-scale bubbling fluidized bed reactor under standard CLC operating conditions using room temperature feed gasses. The concept of a cluster of GSC reactors capable of delivering two steady outlet process streams to the downstream power cycle is also discussed.

3 Experiments

Gas Switching Combustion (GSC) is a novel reactor concept based on the standard CLC concept, where the difference is that GSC uses a single fluidized bed reactor instead of the interconnected fluidized bed reactors used in the standard CLC process (Figure 1). By the use of a switching mechanism, fuel and air streams are fed periodically to the single reactor where the oxygen carrier material undergoes redox reactions.

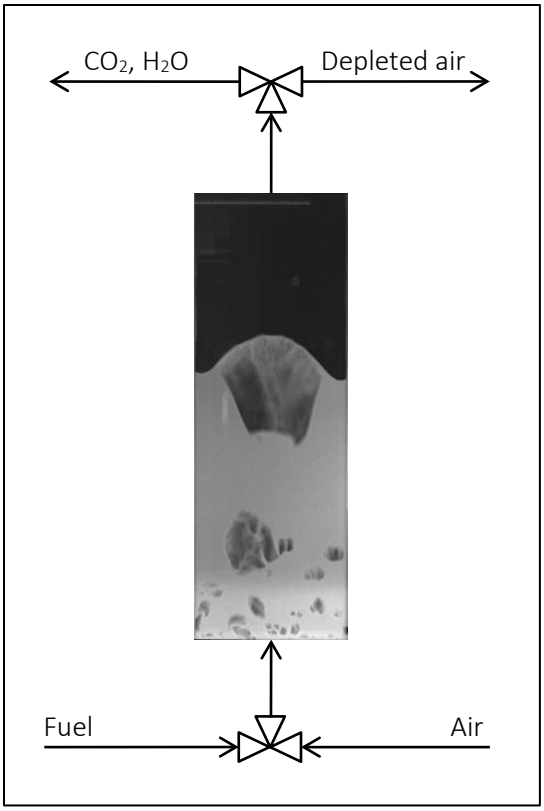

Figure 1: Simple illustration of a GSC reactor. Air and fuel streams enter at room temperature and hot process gasses are delivered to the downstream power cycle and CO_2 drying and compression unit.

3.1 Setup and methodology

The experimental setup (Figure 2) consists of a pseudo-2D vertical column with a height of 1.5 m, a width of 0.3 m and a depth of 0.015 m. The pseudo-2D configuration was selected for the purpose of extracting local experimental data for detailed CFD model validation and was based on a cold flow unit with similar dimensions (27). The reactor column is made from Inconnel 600 in order to withstand the harsh conditions of high temperatures (up to 1000°C) and reacting gas-solid flows. A ceramic porous plate with 40 micron pores and 7 mm thickness is used as the gas distributor. The setup is equipped with four electrical heaters (Thermcraft Inc.) installed on the back of the reactor in order to heat up the reactor to the target temperature. Each of these heaters is controlled separately allowing for full control of the heat supply to the desired region in the reactor. The heaters and the reactor were covered in blanket insulations (5 cm thickness) before being placed in the middle of a metallic box of 44 cm width, filled with a particulate insulation material (vermiculate).

Three mass flow controllers (Bronkhorst BV) are used for feeding gasses to the reactor. The three gas lines gather at a three-way electrical valve installed before reaching the distributor. This three-way electrical valve is used to switch between feed gasses. Nitrogen and fuel are placed on the same line so they can be fed to the reactor simultaneously when required for fuel dilution. The air is placed on a separate line for avoiding any direct contact between air and fuel. A cooler is positioned at the outlet of the reactor to cool down the stream of hot gasses before it is sent to the vent.

Holes for data acquisition were designed and created on the front side of the reactor along the central axial axis and laterally at a height of 0.3 m above the gas distributor. A multi-purpose tube, 0.3 m in length and 0.001 m in diameter, was designed to allow simultaneous measurements of pressure,

temperature and gas composition at any given position. A fine stainless mesh (40 µm opening) was placed tightly at the entrance of each tube to prevent the infiltration of fine particles from the reactor to the tube. The outer end of the tube is connected to a two-way swagelok where a thermocouple (0.3 m length) and a capillary tube are mounted and inserted through the central axis of the tube to reach the reactor internal wall. In this way the temperature and gas composition are measured exactly at the internal wall of the reactor.

Pressure is measured through transducers capable of withstanding a maximum temperature of 250°C. In order to guarantee that hot gasses from the reactor are cooled down sufficiently before reaching the pressure transducer, a 0.25 m non-insulated tube (exposed to room temperature) is placed between the pressure transducer and the multi-purpose measurement tube. The influence of this extra tube length on the average pressure has been tested by measuring the pressure with and without this whole measurement system at ambient temperature. This test confirmed that the measurement system had no influence on the average pressure measurement. The known weight of particles inside the reactor was also used to double-check the accuracy of the pressure measurements.

The gas composition is measured using a Mass Spectrometer from MKS Instruments Inc. and the temperature is measured in each port along the entire front of the reactor using type K thermocouples. All the measurement instruments, flow controlling devices are controlled through a Labview application. The Labview application is also used for data acquisition and storage.

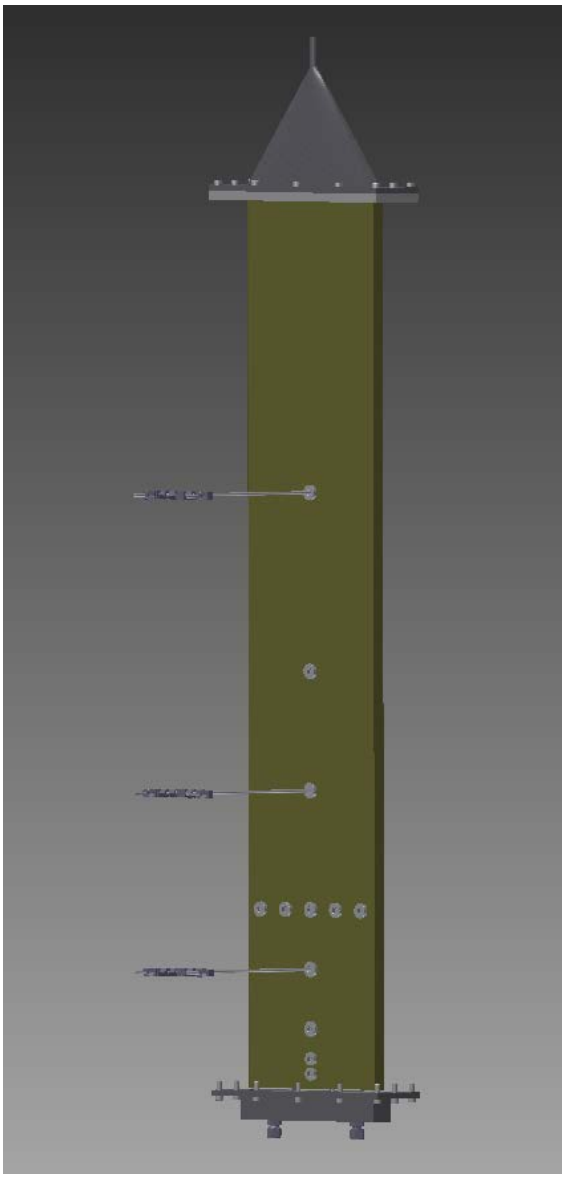

Figure 2: Schematic representative of the experimental set up.

3.2 Operation

All GSC demonstration experiments reported in this paper were completed with an amount of oxygen carrier material corresponding to a 0.3 m static bed height in the reactor. Nickel oxide particles supported on Al_2O_3 (manufactured by VITO) were used as the oxygen carrier. The NiO/Al_2O_3 ratio is 65/35 and the particle size cut-offs D10, D50 and D90 were determined to be 117.4, 161.7 and 231.3 µm respectively. About 37% of the final particle consists of free NiO which is available for reaction. The powder has a loosely packed density of 1950 kg/m^3 and a tapped density of 2166 kg/m^3. This oxygen carrier was selected because it has been successfully used in previous studies (28, 29).

Carbon monoxide was used as a fuel gas in the reduction stage and air was used for oxidation and further heat recovery after the oxygen carrier became fully oxidized. CO was selected in order to avoid uncertainties resulting from the side reactions which take place when CH_4 reacts with Ni-based oxygen carriers. Five seconds purging with pure N_2 was applied between the air and the fuel stages to avoid direct contact between fuel and air and thereby eliminate the risk of explosion.

Experiments were carried out over four autothermal redox cycles after the heaters are switched off. The autothermal operation during the first cycle might be faked by the heat flowing from the heaters which are still storing heat from long heating operation. The measured parameters however were averaged over the last three cycles for each case investigated in this paper. More specifically, the experimental procedure involved the following steps:

1) The heaters are used to reach a pre-specified starting temperature. This "target temperature" is the first of two independent variables investigated in this study.
2) Once the target temperature is reached, the heaters are switched off before the fuel is fed into the reactor for a period of time (called the "fuel time" for the remainder of the paper). The fuel time is the second independent variable under investigation. Reactor temperature stays relatively constant in this stage as the slightly exothermic reaction balances the heat removed by the cold fuel gas.
3) Following the fuel stage, air is fed into the reactor at the same gas flow rate as that used in the fuel stage. During this stage, the bed temperature rises sharply due to the highly exothermic oxidation reaction. This temperature rise continues until the oxygen carrier is almost fully oxidized by which time the reactor starts to cool again as the reaction slows and the cold air continues to remove heat from the system.
4) This cooling part of the oxidation stage is continued until the reactor temperature returns to the target temperature at which point the oxygen carrier is expected to once again be fully oxidized and the next redox cycle is started (point 2 above).

Experiments were performed by varying the two independent variables; the target temperature and the fuel time. Various dependent variables were extracted from each experiment: the CO_2 purity, the CO_2 capture efficiency, the amount of carbon deposition, the maximum temperature variation and the oxidation/reduction time ratio (henceforth called the oxi/red time ratio). These variables will be further discussed in Section 4.1.2. All dependent variables are averaged over the three complete redox cycles. The oxidation stage will henceforth be referred as the OXI phase to avoid any confusion as it includes the oxidation and the heat removal phases

Throughout the study, all temperature measurements are taken at 0.2 m in the central axis of the reactor. Temperature variations at this point are followed throughout the experiment and used to determine the start and end of the redox cycles. Gas species measurements are taken at a height of 0.7 m which is a point in the freeboard well above the expanded bed. These measurements are used to determine the CO_2 purity and capture efficiency as well as the carbon deposition.

The superficial gas velocity is kept constant at 0.3 m/s ($U/Umf \approx 14$ when air is used as a fluidizing gas at 700 °C) for all the experiments during both the air and the fuel stages. Therefore, the gas mass flowrate is recalculated each time the bed temperature is changed in order to set the superficial gas velocity to 0.3 m/s. The pressure along the height of the reactor is measured regularly in order to quantify the bed weight and to inspect any unexpected loss of particles caused by elutriation of particles due to gas expansion when the reactor reaches higher temperatures.

3.3 Mass and energy balance

The mass of the oxygen carrier placed originally in the reactor is 2.63 kg and contains 37% active NiO. A total of 13.03 moles of active materials is therefore available for reaction.

As discussed above, the process gasses were fed to the reactor at a flowrate resulting in a superficial fluidization velocity of 0.3 m/s at the given target temperature. For example, the molar flowrate at which pure CO fuel would be introduced at 700°C would be

$$\dot{n}_{CO} = \frac{P\left(u_{CO}A\right)}{RT} = \frac{101325 \times 0.3 \times 0.3 \times 0.015}{8.314 \times 973.15} = 0.0169 \text{ mol/s}.$$

Since CO and NiO react in a 1:1 stoichiometric ratio, 771 s of CO feed is required to fully convert the oxygen carrier material (13.03 moles) at a target temperature of 700°C.

For determining the length of the air stage, an energy balance is required because the air stage first fully oxidizes the material and then proceeds to remove the excess heat until the reactor temperature returns to the target. In order to simplify this calculation, it will be assumed that CO and air have similar physical properties and that the heat capacity of the gasses can be approximated at a constant value of 1.1 kJ/(kg.K).

When CO is combusted in air, 283 kJ/mol of heat is released. Thus, assuming an average temperature rise of 700°C in the feed gasses and an adiabatic reactor, the following mass of ambient feed gasses is required to balance the net heat release by the reaction:

$$m_g = \frac{n_{NiO}H_{rxn}}{c_{p,g}\Delta T}x_{red} = \frac{13.03 \times 283}{1.1 \times 700}x_{red} = 4.79x_{red} \text{ kg}$$

Here, x_{red} represents the fraction by which the oxygen carrier was reduced during the reduction stage. Assuming that $x_{red} = 1$ for complete reduction of the oxygen carrier, 4.79 kg of feed gasses will be required to remove the heat released by the combustion of CO. Assuming that CO shares the physical properties of air, the gasses will have a density of 0.363 kg/m^3 at 700°C, implying that 13.19 m^3 of gas or 9769.6 s of fluidization at a superficial velocity of 0.3 m/s will be required.

Since 771 s of this time is used by the reduction stage, the oxidation (and heat removal) stage will be 8998.6 s long (11.67 times longer than the reduction stage). As will be discussed later in this paper, however, such a high ratio between the oxidation and reduction stage times cannot be achieved in practice due to substantial heat losses.

4 Results and discussion

Results will be presented and discussed in two sections: the demonstration of autothermal operation of the GSC reactor (Section 4.1) and a parametric study to evaluate the sensitivity of the reactor performance to changes in the two independent variables (Section 4.2). Finally, a discussion on the application of the GSC reactor concept in a real plant will be presented.

4.1 Demonstration of the GSC concept

4.1.1 Temperature evolution

The transient temperature profile at three axial positions inside the reactor (0.05 m, 0.1 m and 0.2 m) over three redox cycles while the heaters are switched off is depicted in Figure 3. The results show a repeatable temperature evolution cycle at each axial position during the three redox cycles performed

and therefore demonstrates that the GSC reactor can be operated autothermally using a periodic cycling of room temperature feed gasses.

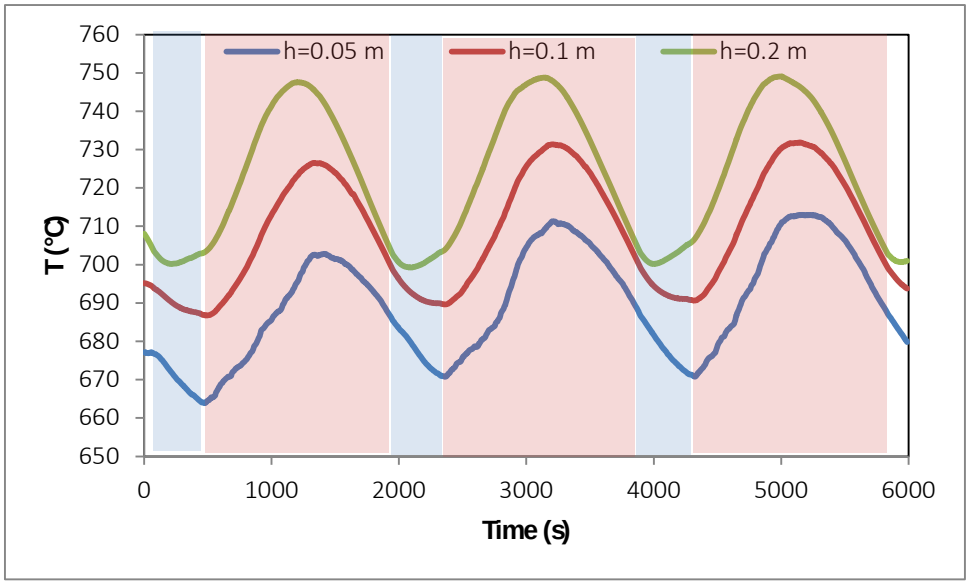

Figure 3: Temperature evolution over three redox cycles at three axial positions on the reactor centreline. The experiment was performed with a fuel time of 6 minutes and target temperature of 700°C.

The results also show the existence of an axial temperature gradient where the gas undergoes a 30-40°C temperature increase when it moves up from 0.05 m to 0.2 m. It is expected that this temperature gradient is due to heat losses at the bottom of the reactor and poor axial mixing of solids caused by the large frictional shear stresses imposed by the large front and back walls in the pseudo-2D reactor (see the PIV measurements compared to simulations carried out with frictionless walls in a previous cold model study (27)). Both of these issues can be easily fixed by simple design changes. However, optimization of the reactor configuration and operating conditions is out of the scope of the present study.

4.1.2 Reactor performance

The performance of the GSC concept is assessed based on the quantification of the following dependent variables:

- CO_2 capture efficiency. This was calculated by determining the percentage of the total produced CO_2 (calculated assuming 100% conversion of the incoming CO) which exited in the outlet gas over the entire OXI stage. The CO_2 capture efficiency was then taken as 100% minus the percentage of CO_2 that escaped to the atmosphere with the depleted air. Naturally, a high degree of CO_2 capture is desired in order to keep greenhouse gas emissions minimal.
- CO_2 purity. This was calculated by determining the amount of depleted air and CO present in the outlet stream over the entire reduction stage. The CO_2 purity was then taken as 100% minus the percentage of impurities (depleted air and CO) in the reduction stage outlet stream which would be sent to compression and storage in a real plant. Naturally, a high CO_2 purity is desired so that the volume of gas to be compressed, transported and stored is kept to a minimum.
- Carbon deposition. The Boudouard carbon deposition reaction ($2CO \rightarrow CO_2 + C$) can occur on the Ni-based oxygen carrier (employed in this study) in the reduction stage and then reacts with oxygen in the OXI stage to be released to the atmosphere as CO_2. This is an undesired

phenomenon and it was quantified as the molar ratio of the total amount of CO_2 released during the air stage and the total amount of CO fed to the reactor during the fuel stage. Carbon deposition was measured in a separate cycle where a long purging stage with nitrogen was applied after the reduction stage. This eliminated CO_2 leakage and ensured that all CO_2 measured during the subsequent OXI stage could be safely attributed to combustion of the deposited carbon.

- Temperature rise. Due to the transient cycling operation of the reactor, the reactor temperature will vary throughout the cycle (Figure 3). It is important that this variation is not so large that lower temperatures cause incomplete fuel conversion or higher temperatures damage the reactor or downstream equipment. The difference between the maximum and minimum temperatures in the redox cycle will therefore be recorded in each experiment.
- Oxi/red time ratio. The OXI stage will be significantly longer than the fuel stage if constant flowrates are used both because the molar density of oxygen in air is lower than the molar density of the pure CO fuel and because a large amount of heat must be removed from the system by the cold air after the oxygen carrier has been fully oxidized. The ratio between the OXI stage time and the reduction stage time will therefore be recorded for each experiment.

In the demonstration experiment, these dependent variables were measured at a target temperature of 700°C and a fuel time of 6 minutes. Results are presented in Table 1.

Table 1: Reactor performance parameters data for the case of 6 min fuel time and target temperature of 700 °C.

Cycle	CO_2 capture efficiency (%)	CO_2 purity (%)	Carbon deposition (%)	Temperature rise (°C)	Oxi/red time ratio
1	96.36	98.36	-	42.8	4.13
2	97.13	98.08	-	48.6	4.33
3	96.37	98.29	-	47.1	4.29
Average	96.63	98.24	0.87	46.17	4.25

The high CO_2 capture efficiency achieved in Table 1 is very encouraging. The 96.63% CO2 capture efficiency implies that only 3.37% of the CO_2 formed would be released to the atmosphere in the actual plant. In the GSC concept, this small amount of escaped CO_2 is caused by two factors: 1) the temporary mixing of CO_2 and air when switching from the fuel stage to the air stage and 2) the contribution from the carbon deposition phenomenon (the Boudouard reaction: $2CO \rightarrow CO_2 + C$). Results show that roughly 0.87% of the 3.37% leaked CO_2 resulted from the OXI of the carbon deposited on the oxygen carrier. This means the degree of undesired mixing when switching from the reduction to the OXI stage was only about 2.5%. If desired, this leakage could be completely eliminated by purging with a suitable gas between each stage to ensure no contact between CO_2 and N_2, but the added complexity and cost associated with such an addition will probably be unwarranted. This decision will ultimately depend on plant economics, especially the price of CO_2 and the added capital and operational costs associated with the extra purging stage.

The CO_2 purity is also very high with only 1.76% of the fuel stage outlet stream consisting of unwanted N_2, O_2 and CO. Since the fuel conversion was essentially 100%, the impurities in the CO_2 stream primarily consist of N_2 and O_2 from the OXI stage. This gas leakage is comparable to the leakage reducing the CO_2 capture efficiency discussed above, implying that the degree of undesired mixing is similar. This leakage could theoretically also be eliminated by an added purging stage between OXI and reduction.

If the purging stage is excluded (as in this study) it is also possible to trade a higher CO_2 capture efficiency for a lower CO_2 purity and vice versa. In this study, it was assumed that the outlet gasses were switched whenever the CO_2 volume fraction crossed 0.5. In other words, when the inlet gasses were switched from air to fuel, it was assumed that the outlet gasses would be switched when the CO_2 mole fraction increased to 0.5. Similarly, when the inlet gasses were switched from fuel to air, it was assumed that the outlet gasses would be switched when the CO_2 mole fraction decreased to 0.5. This is illustrated in Figure 4.

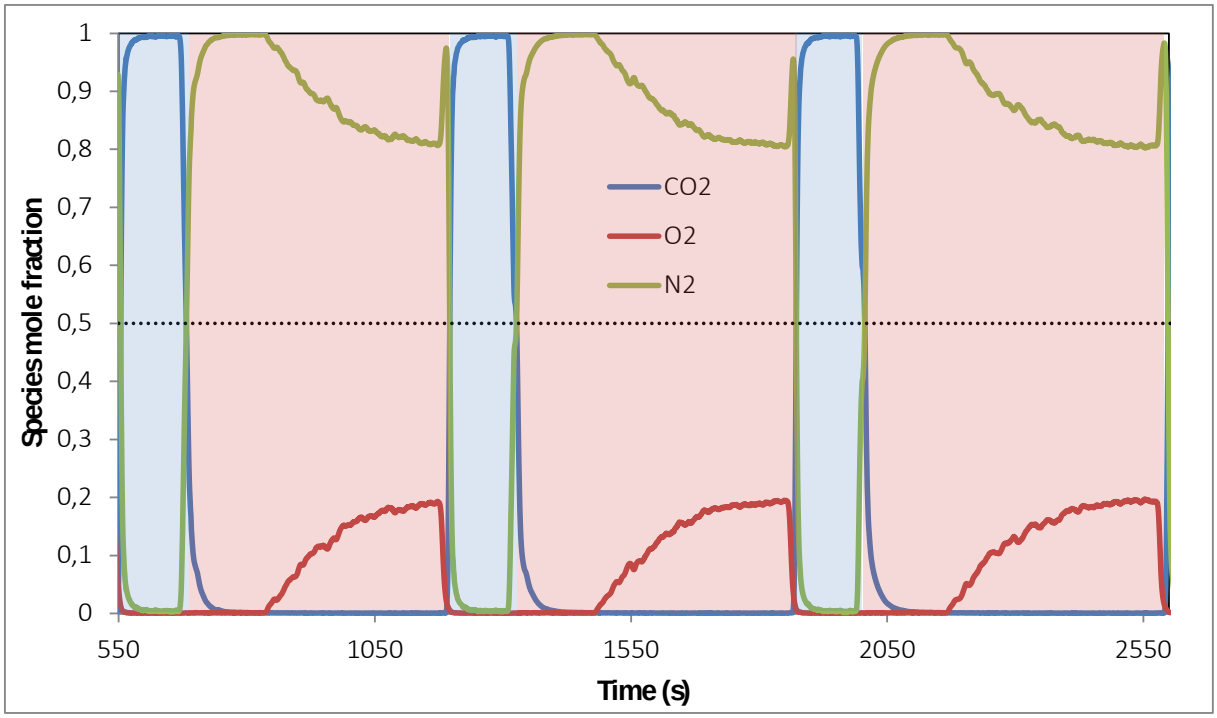

Figure 4: Transient evolution of the gas species concentrations in the freeboard (0.7 m above the distributor) at a target temperature of 700°C and a fuel time of 2 minutes. The blue shaded areas represent the time when gasses would be sent to compression and storage and the red shaded areas represent the time when gasses would be vented to the atmosphere (in a full power plant).

If, for example, economic considerations show that it is more efficient to compress and store some additional impurities with the CO_2 stream than it is to emit CO_2 to the atmosphere (a high CO_2 capture efficiency is more important than a high CO_2 purity), the timing of the switch in outlet gasses can be changed accordingly. In this example, the outlet gas switch would be made a few seconds later following the inlet gas switch from fuel to air and a few seconds earlier following the inlet gas switch from air to fuel.

When looking at the temperature rise in Table 1, a fairly moderate rise of 46.17°C is observed. This transient variation in temperature is unlikely to have any negative effects on the reactive performance or the downstream process equipment in a full power plant. In addition, as will be discussed in Section 4.3, a cluster of reactors can eliminate much of the transient temperature variation seen by the downstream power cycle, thereby ensuring virtually steady operation.

Finally, the oxi/red time ratio of 4.25 implies that the time needed for the OXI stage to fully oxidize the oxygen carrier material and cool down the bed was about 25.5 minutes. This oxi/red time ratio is much smaller than the adiabatic value of 11.67 calculated in Section 3.3, implying that large heat losses are

occurring from the reactor. Naturally, such heat losses must be minimized in a real plant in order to maximize the power output.

To summarize, the GSC concept could be operated autothermally and shows good performance as a CO_2 capture technology for power generation. CO_2 capture efficiency and purity were high, carbon deposition was low and transient temperature variations over the redox cycle were moderate. Heat losses from the reactor were large, but this can easily be greatly reduced by building a large reactor (higher volume/surface ratio) and applying more insulation.

4.2 Parametric study

4.2.1 Sensitivity to the fuel time

In this parametric study, the fuel time was varied between 1 minute and 8 minutes while the target temperature was kept constant at 700°C. Results are displayed in Figure 5 and Figure 7.

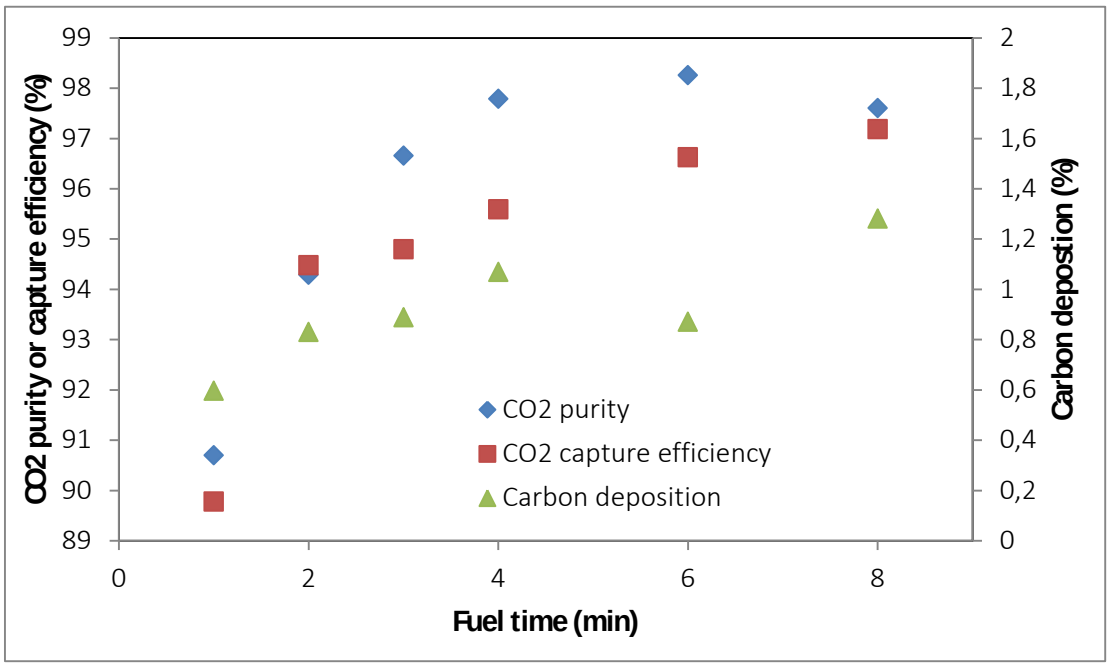

Figure 5: Sensitivity of the CO_2 capture efficiency, CO_2 purity and carbon deposition to changes in the fuel time. The target temperature is kept constant at 700 °C.

As shown in Figure 5, the CO_2 capture efficiency and purity increased with increases in the fuel time. This is to be expected because the short period of undesired gas mixing after each feed gas switch progressively reduces in significance as the fuel time (and therefore also the air time) increases. It is therefore desirable to ensure that the fuel time is as long as possible. The maximum length of the fuel time will be limited by the oxygen carrying capacity and total inventory of oxygen carrier material, the reduction in oxygen carrier reactivity with increasing reduction (further discussed under Figure 6) and possibly by the transient temperature variations (further discussed under Figure 7).

Figure 5 also shows that the amount of carbon which deposits on the oxygen carrier during the fuel stage is quite small (0.6-1.3%). Despite the slow increase in carbon deposition with fuel time, the CO_2 capture efficiency still increases due to the mechanism discussed above. It is expected, however, that further increases in the fuel time will cause great increases in the amount of carbon deposition. For

example, Cho *et al.* (30) found that carbon deposition suddenly increases dramatically as the NiO oxygen carrier is reduced more than 80%.

One slight anomaly in Figure 5 is the lower CO_2 purity for the 8 minutes fuel time. The reason for this unexpected decrease is shown in Figure 6 where it becomes apparent that some CO fuel starts to slip through the bed during the last two minutes of the reduction stage. Since such fuel slippage is highly undesirable, this case clearly illustrates one of the limitations to the length of the cycle time outlined above. From the calculations in Section 3.3, 8 minutes of reduction at 100% CO conversion would result in 62.2% reduction of the oxygen carrier, implying that the reaction rate will be significantly lower and that significant carbon deposition could occur upon further reduction. This amount of fuel slip at 62.2% conversion also depends on the temperature selected for the experiment. Higher temperatures (also required for higher plant efficiency) would result in higher reaction rates and lower carbon deposition, making it possible to achieve higher conversions and thus longer cycle times.

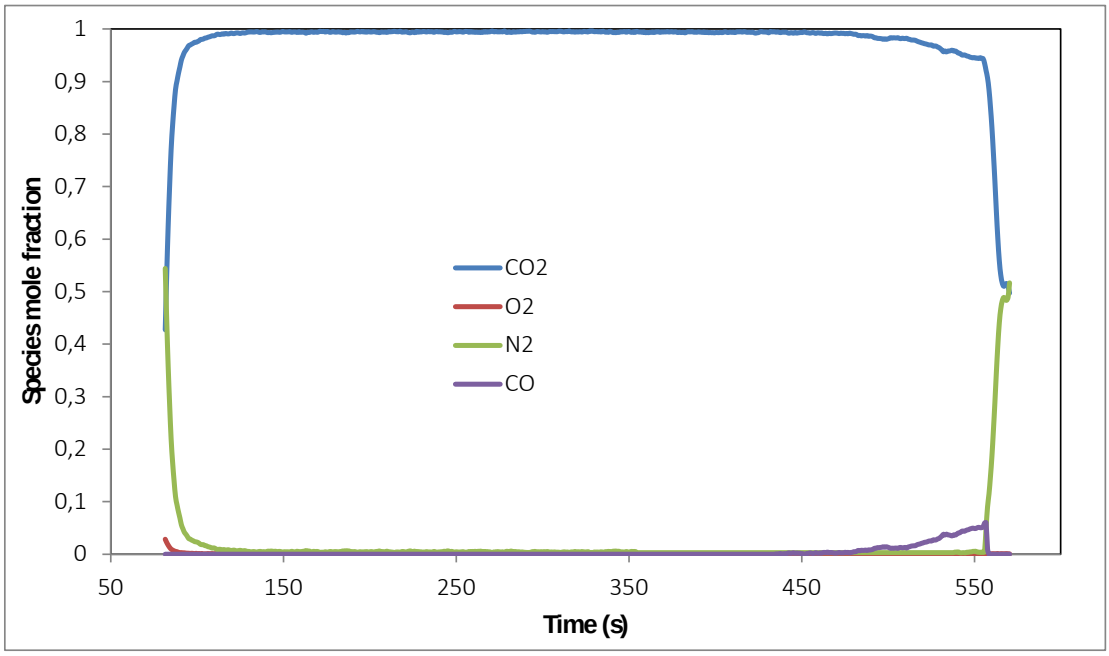

Figure 6: Transient evolution of the gas species concentrations in the freeboard (0.7 m above the distributor) at a target temperature of 700°C and a fuel time of 8 minutes. Only one reduction stage is shown. It should also be noted that CO and N_2 are measured as one species by the mass spectrometer (due to similar molar weights) and that the distinction made in this graph is based on an understanding of when these two species will be present during the GSC cycle.

When inspecting Figure 7, the expected trend of increasing temperature rises with increasing fuel times is observed. In an adiabatic system where fuel conversion is always 100%, the temperature rise should increase linearly with the fuel time, but in this case, a slight logarithmic tendency is observed towards higher fuel times. This is due to larger heat losses (through the reactor walls) at higher temperature rises and also due to the incomplete fuel conversion observed for the 8 minute fuel time in Figure 6.

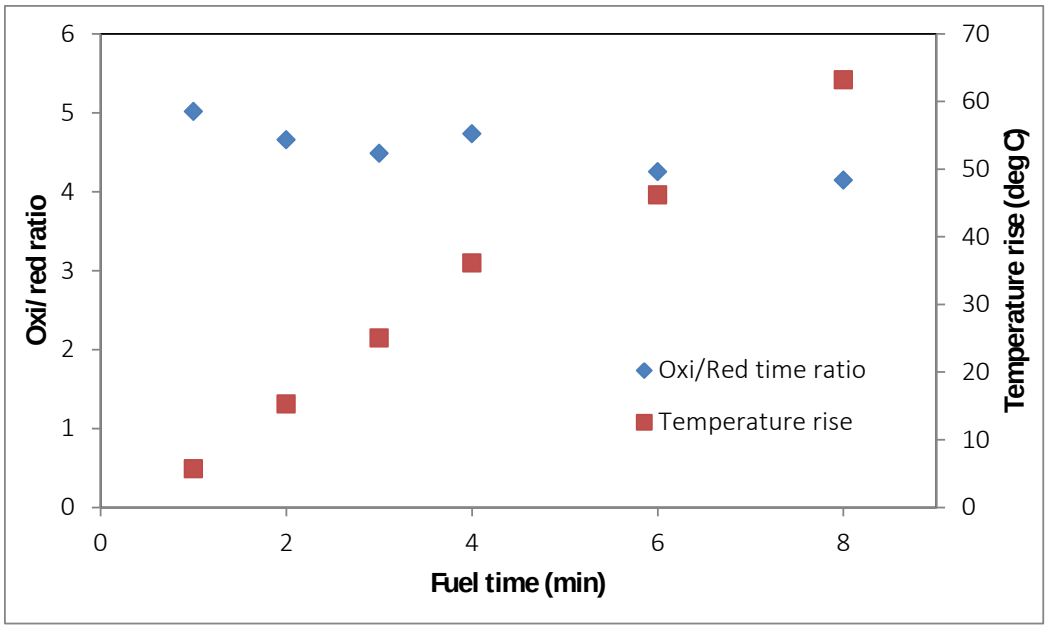

Figure 7: Sensitivity of the oxi/red time ratio and the temperature rise to changes in the fuel time. The target temperature is kept constant at 700°C.

Figure 7 shows that the oxi/red time ratio is not as sensitive to changes in the fuel time. The 20% decrease in the oxi/red time ratio as the fuel time is increased from 1 minute to 8 minutes can be attributed to increases in the average temperature throughout the cycle as the temperature rise increases greatly. Higher fuel times will therefore result in greater rates of heat loss and heat removal which will require less time for the cold air stream to cool the reactor back down to the target temperature.

4.2.2 Sensitivity to the target temperature

This parametric study is carried out for target temperatures ranging from 500 to 760°C while keeping the fuel time constant at 4 minutes. Results are presented in Figure 8 and Figure 9.

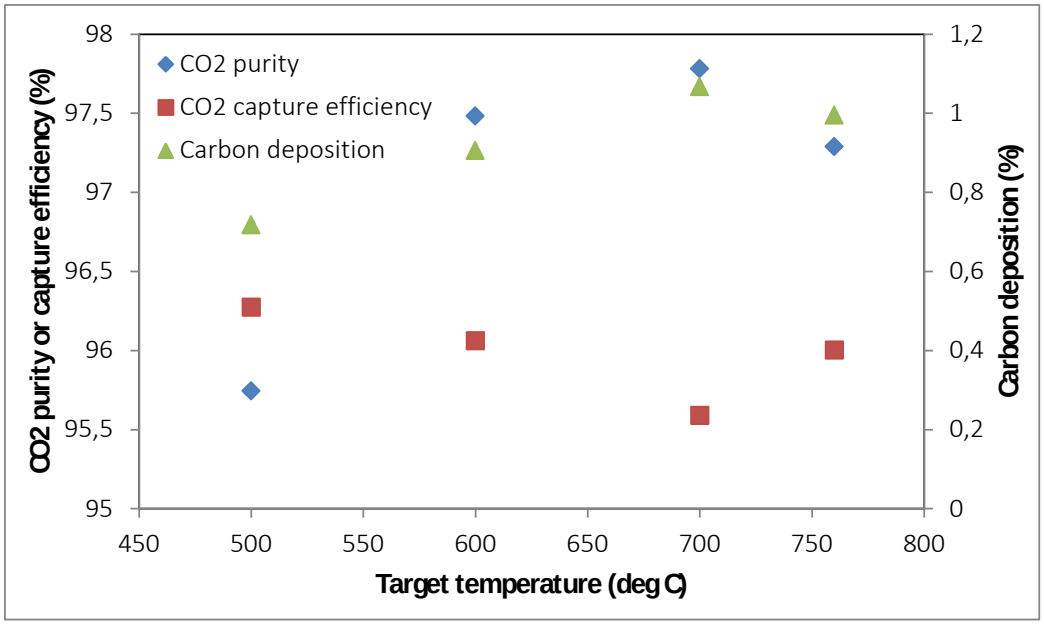

Figure 8: Sensitivity of the CO_2 capture efficiency, the CO_2 purity, and the carbon deposition to changes in the target temperature. The fuel time is kept constant at 4min.

When looking at Figure 8, it is observed that the CO_2 capture efficiency and purity are fairly constant across the range of target temperatures with the notable exception being the CO_2 purity at a target temperature of 500°C. For the remaining three cases, the carbon deposition (which is also fairly constant over the target temperatures investigated) appears to explain most of the difference between the CO_2 capture efficiency and purity. The reason for the lower CO_2 purity at 500°C is a relatively constant fuel slippage (around 2%) throughout the reduction stage. A target temperature of 600°C therefore appears to be the minimum that can be afforded by this particular setup before the reaction rate slows down sufficiently to result in significant amounts of undesired fuel slippage.

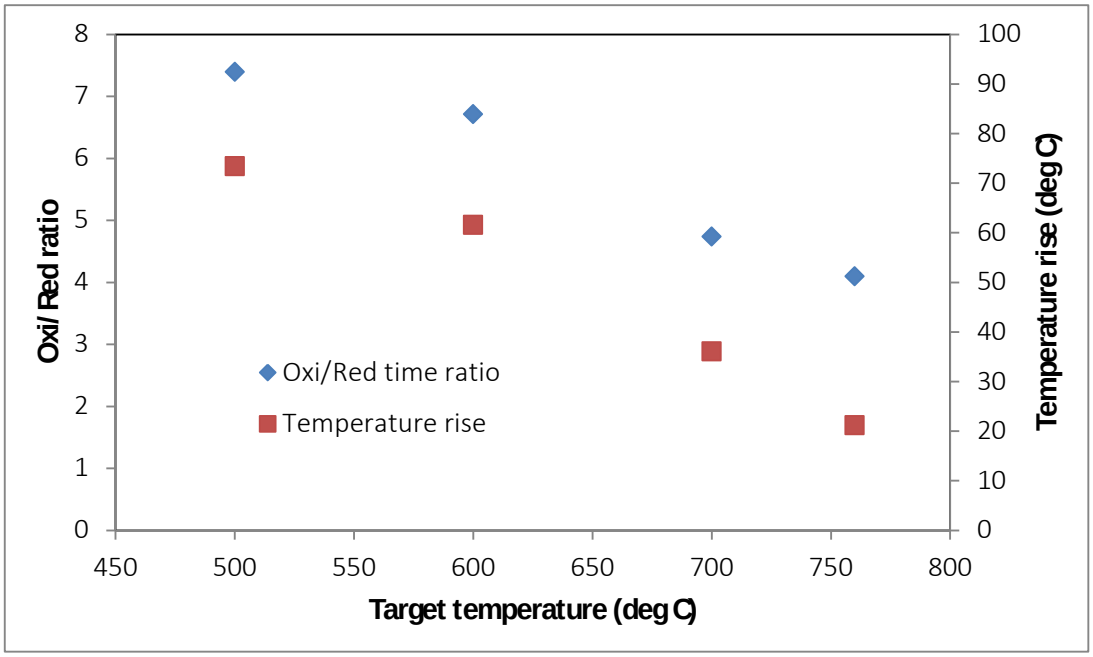

Figure 9: Sensitivity of the oxi/red time ratio and the temperature rise to changes in the target temperature. The fuel time is kept constant at 4 minutes.

Figure 9 shows a marked decline both in the temperature rise and the oxi/red time ratio as the target temperature is increased. Both of these rapid reductions can be explained by a rapid deterioration of the efficiency of the insulation material as the target temperature is increased. This large sensitivity of the heat losses to the reactor temperature indicates that radiative heat transfer might be dominant in the particulate medium used for the majority of insulation. Radiation increases rapidly with an increase in temperature and such radiative heat transfer from one particle to the next in the insulation material would explain the strong damping in the temperature rise with increasing target temperatures observed in Figure 9.

Another factor influencing the strong trend in the temperature rise is the decrease in the mass of CO fed to the reactor as the target temperature is increased. Since the superficial gas velocity and the fuel time was kept constant across all runs, the mass of CO fed to the reactor decreased by 25% as the target temperature was increased from 500 to 760°C (due to the gas density decrease). Finally, increases in the target temperature would also increase the rate at which cold inlet gasses extract heat from the system, thereby decreasing the temperature rise and the oxi/red time ratio.

4.3 Steady operation using a cluster of GSC reactors

The results presented in the previous sections demonstrated the autothermal operation of a GSC reactor. In other words, it was shown that the GSC concept could, on an alternating basis, supply a hot CO_2-rich stream and a hot CO_2-lean stream to a downstream power cycle and CO_2 compression facility. However, a single GSC reactor is not able to deliver the continuous process streams required by these downstream processes. In order to overcome this drawback, a cluster of multiple GSC reactors could be employed and operated in such a way that two continuous streams of hot process gasses are delivered to downstream process equipment. A simple illustration of such a cluster is shown in Figure 10.

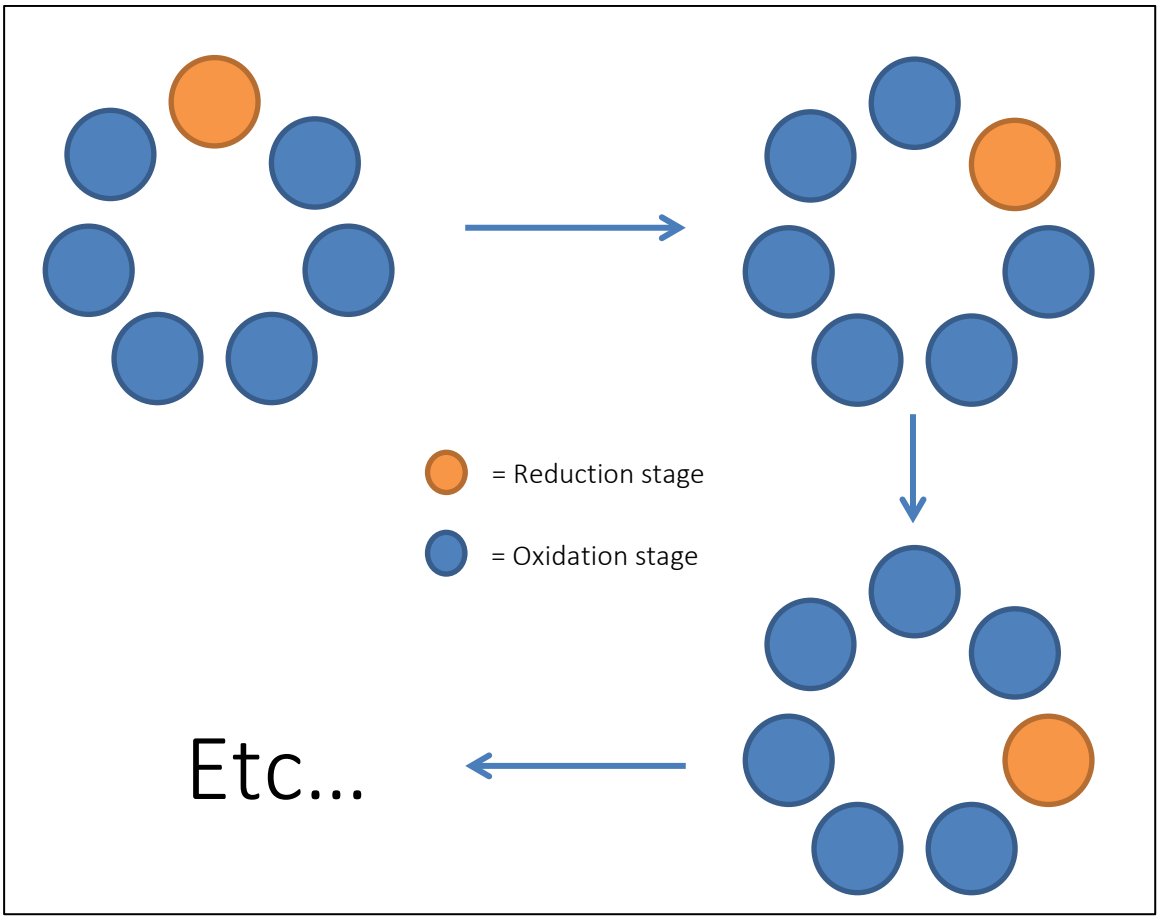

Figure 10: Illustration of the operation of a cluster of GSC reactors designed to achieve near-steady state operation. Each disc represents one reactor.

It is shown that, at any given point in time, multiple reactors are operating in OXI mode while only one is operating in reduction mode. This is to allow for the high oxi/red time ratio of the process which implies that, if the fuel and air flowrates are similar, the OXI stage will have to be much longer than the reduction stage in each GSC reactor. Alternatively, only two reactors can be used in the cluster and the fuel flowrate could be reduced accordingly, but this option could be less economical. For example, if the cluster of seven reactors in Figure 10 were to be reduced to only two by reducing the fuel feed rate, the plant power output would drop by a factor of 6, while the number of reactors (and hence the capital expenses) would only drop by a factor of 3.5. Further studies will strive to quantify the economic implications of this important design consideration.

An additional advantage of having a larger cluster is that all reactors operating in OXI mode at any given time will be at different stages of OXI and therefore at different temperatures. The outlet streams from these reactors will be mixed before reaching the power cycle to result in a relatively uniform stream temperature. As seen in Figure 5, larger fuel times are desirable because they ensure higher CO_2 capture efficiencies and purities, but Figure 6 also shows that these longer fuel times cause greater transient temperature variations throughout the OXI stage. This mechanism of mixing output streams from several reactors will claim the benefit of long stage times while avoiding much of the penalty imposed by large temperature rises.

The oxi/red time ratio evaluated in this study becomes a very important parameter in the operation of such a cluster of GSC reactors. The correct number of reactors in the cluster will always be the oxi/red time ratio plus one. In Figure 10, for example, the oxi/red time ratio is 6 and the total number of reactors is 7. It is therefore mandatory that the cluster must be operated in such a way that the oxi/red time ratio is an integer. This will be most conveniently done by ensuring that the gas flow rate used under OXI is at the maximum and then lowering the fuel flow rate under reduction slightly so as to reduce the oxi/red time ratio to the nearest integer value.

Finally, it should be mentioned that the valve control system necessary for controlling such a cluster of GSC reactors will add some complexity and cost to the system (especially for the hot outlet streams). It is reasoned, however, that this negative aspect is greatly outweighed by several positives such as easier scale-up, easier process control, easier pressurized operation and improved heat integration. More experience and an energy analysis of the whole power plant will be required to make a better judgement regarding the potentials of the GSC concept relative to the well-established CLC concept.

5 Summary and conclusions

This study has successfully demonstrated the Gas Switching Combustion (GSC) reactor concept for power generation with integrated CO_2 capture. As an alternative to the standard CLC process, the GSC concept uses a single dense fluidized bed reactor and alternatively exposes the oxygen carrier material to fuel and air in order to avoid direct contact between CO_2 and N_2.

In order to demonstrate the concept, a lab-scale GSC reactor was operated autothermally using cold feed gasses to produce hot outlet gasses which would be suitable for use in a downstream power cycle. The effect of two independent variables; the target temperature and the fuel time, were investigated in this study. The target temperature was the set point at which the reduction stage in each redox cycle was commenced and the fuel time was the time for which fuel was fed to the reactor at a fixed fluidization velocity.

Results were encouraging and showed high CO_2 capture efficiencies (up to 97.2%) and CO_2 purities (up to 98.2%) when the fuel time was long (6-8 minutes). These results were achieved without the use of a purge stage between the oxidation and reduction stages, implying that the CO_2 capture efficiency and purity could be improved by including such a purging stage. However, it is doubtful whether the one or two percentage point improvement offered by this strategy would be worth the added complexity and cost of two additional purging stages in each redox cycle.

The NiO oxygen carrier used also experienced some carbon deposition when reduced by the CO fuel. The amount of carbon deposition was generally small (around 1%), however, and therefore did not have a large effect on the CO_2 capture efficiency.

Another feature of the GSC concept is the transient temperature variation in the reactor as the oxygen carrier gets reduced (endothermic), oxidized (exothermic) and then cooled back to the target temperature. The magnitude of this transient temperature variation is an important parameter which must not become too large. The maximum value found in this study was 73.4°C at the lowest target temperature (500°C). Relatively poor performance of the reactor insulation material at higher temperatures damped the transient temperature rise, however, and this value would therefore be of greater influence in a better insulated reactor.

Finally, the ratio between the fuel time and the air time (a variable termed the oxi/red time ratio) was investigated. The OXI stage (air time) was much longer than the reduction stage (fuel time) because the molar density of the air feed was lower than that of the fuel feed and the air feed is also used to cool the bed back down to the target temperature once oxidation is complete. The oxi/red time ratio was again influenced greatly by the heat losses from the reactor and reached a maximum value of 7.4 at the lowest temperature investigated (where the heat losses were lowest).

The study also briefly discussed the concept of a cluster of GSC reactors operating in such a way that two steady process streams are sent to downstream process equipment. This GSC cluster concept has some notable advantages over the standard Chemical Looping Combustion (CLC) process for power production with integrated CO_2 capture. These advantages include a substantial reduction in process complexity (much easier scale-up), no transport of solids (no need for external particle separation and loop seal equipment), the possibility of high pressure operation (the standalone GSC reactors are much simpler to pressurize than the complete CLC loop), and better heat integration (the solids remain in a single reactor, thereby directly transferring heat from one reactor stage to the next).

To conclude, the GSC reactor concept proved to be a simple and effective way of power production with integrated CO_2 capture and could greatly accelerate the progress of CLC-type CO_2 capture technologies. Further scale-up studies and energy analysis are recommended.

6 Acknowledgements

The authors would like to acknowledge the funding received from the Research Council of Norway which enabled the completion of this work. Joost Kors is acknowledged for constructing and maintaining the experimental setup.

7 References

1. Maddison, A., *Historical Statistics of the World Economy: 1-2008 AD*. 2008.
2. BP, *Statistical Review of World Energy*. 2012.
3. BP, *Energy Outlook 2030*. 2013.
4. IEA, *World Energy Outlook 2012*. 2012, International Energy Agency.
5. EIA, *International Energy Outlook 2011*. 2011, US Energy and Information Administration.
6. Mobil, E., *The Outlook for Energy*. 2012.
7. IPCC, *Climate Change 2007: Mitigation of Climate Change*. 2007, Cambridge University Press.

8. Butt, T.E., R.D. Giddings, and K.G. Jones, *Environmental sustainability and climate change mitigation-CCS technology, better having it than not having it at all!* Environmental Progress & Sustainable Energy, 2012. **31**(4): p. 642-649.
9. Metz, B., et al., *Carbon Capture and Storage*. 2005, Intergovernmental Panel on Climate Change.
10. Lyngfelt, A., B. Leckner, and T. Mattisson, *A fluidized-bed combustion process with inherent CO2 separation; application of chemical-looping combustion.* Chemical Engineering Science, 2001. **56**(10): p. 3101-3113.
11. Hossain, M.M. and H.I. de Lasa, *Chemical-looping combustion (CLC) for inherent CO2 separations-a review.* Chemical Engineering Science, 2008. **63**(18): p. 4433-4451.
12. Adanez, J., et al., *Selection of oxygen carriers for chemical-looping combustion.* Energy & Fuels, 2004. **18**(2): p. 371-377.
13. Ishida, M., D. Zheng, and T. Akehata, *Evaluation of a chemical-looping-combustion power-generation system by graphic exergy analysis.* Energy, 1987. **12**(2): p. 147-154.
14. *Oxy Combustion with CO2 Capture*, in *CO2 Capture Technologies*. 2012, Global CCS Institute.
15. Ekström, C., et al., *Techno-Economic Evaluations and Benchmarking of Pre-combustion CO2 Capture and Oxy-fuel Processes Developed in the European ENCAP Project.* Energy Procedia, 2009. **1**(1): p. 4233-4240.
16. Abad, A., et al., *Reduction kinetics of Cu-, Ni-, and Fe-based oxygen carriers using syngas (CO + H-2) for chemical-looping combustion.* Energy & Fuels, 2007. **21**(4): p. 1843-1853.
17. Zafar, Q., et al., *Reaction kinetics of freeze-granulated NiO/MgAl2O4 oxygen carrier particles for chemical-looping combustion.* Energy & Fuels, 2007. **21**(2): p. 610-618.
18. Ding, N., et al., *Development and Testing of an Interconnected Fluidized-Bed System for Chemical Looping Combustion.* Chemical Engineering & Technology, 2012. **35**(3): p. 532-538.
19. Kronberger, B., et al., *A two-compartment fluidized bed reactor for CO2 capture by chemical-looping combustion.* Chemical Engineering & Technology, 2004. **27**(12): p. 1318-1326.
20. Johansson, E., et al., *A 300 W laboratory reactor system for chemical-looping combustion with particle circulation.* Fuel, 2006. **85**(10-11): p. 1428-1438.
21. Linderholm, C., et al., *160 h of chemical-looping combustion in a 10 kW reactor system with a NiO-based oxygen carrier.* International Journal of Greenhouse Gas Control, 2008. **2**(4): p. 520-530.
22. Proll, T., et al., *Chemical Looping Pilot Plant Results Using a Nickel-Based Oxygen Carrier.* Oil & Gas Science and Technology-Revue D Ifp Energies Nouvelles, 2011. **66**(2): p. 173-180.
23. Noorman, S., et al., *Experimental Investigation of Chemical-Looping Combustion in Packed Beds: A Parametric Study.* Industrial & Engineering Chemistry Research, 2011. **50**(4): p. 1968-1980.
24. Noorman, S., M. van Sint Annaland, and Kuipers, *Packed Bed Reactor Technology for Chemical-Looping Combustion.* Industrial & Engineering Chemistry Research, 2007. **46**(12): p. 4212-4220.
25. Hamers, H.P., et al., *A novel reactor configuration for packed bed chemical-looping combustion of syngas.* International Journal of Greenhouse Gas Control, 2013. **16**(0): p. 1-12.
26. Spallina, V., et al., *Investigation of heat management for CLC of syngas in packed bed reactors.* Chemical Engineering Journal, 2013. **225**(0): p. 174-191.
27. Cloete, S., et al., *The generality of the standard 2D TFM approach in predicting bubbling fluidized bed hydrodynamics.* Powder Technology, 2013. **235**: p. 735-746.
28. Bolhàr-Nordenkampf, J., et al., *Performance of a NiO-based oxygen carrier for chemical looping combustion and reforming in a 120 kW unit.* Energy Procedia, 2009. **1**(1): p. 19-25.
29. Mattisson, T., et al., *Chemical-looping Combustion CO2 Ready Gas Power.* Energy Procedia, 2009. **1**(1): p. 1557-1564.
30. Cho, P., T. Mattisson, and A. Lyngfelt, *Carbon formation on nickel and iron oxide-containing oxygen carriers for chemical-looping combustion.* Industrial & Engineering Chemistry Research, 2005. **44**(4): p. 668-676.